

3rd International Conference on Material and Component Performance
under Variable Amplitude Loading, VAL2015Analysis of variable strain amplitude response caused by impact
loading of carbon nanotube reinforced magnesium alloy AZ31BM.F. Abdullah^b, S. Abdullah^{a*}, M.Z. Omar^a, Z. Sajuri^a, M.S. Risby^b

^a*Department of Mechanical and Materials Engineering,
Faculty of Engineering & Built Environment,
Universiti Kebangsaan Malaysia,
43600 UKM Bangi, Selangor, Malaysia.*

^b*Department of Mechanical Engineering, Faculty of Engineering,
Universiti Pertahanan Nasional Malaysia,
Kem Sg. Besi 57000 Kuala Lumpur, Malaysia.*

Abstract

This paper presents the effects of carbon nanotubes (CNT) in the AZ31B magnesium alloy when loaded by impact tests associated to transient-based variable amplitude (VA) loadings. The failure behaviors of this alloy, as well as the effects of varying percentages of added carbon nanotubes (CNTs) on the absorption energy of the alloys under transient variable amplitude load impact signal were investigated thoroughly via both experiment and simulation. The CNT composition of 0.1, 0.2, and 0.5 by percentage weight of CNT in AZ31B were chosen as the specimen preparation. The Charpy testing was then used to record the impact behavior of the specimens. In addition, a strain gauges was attached on each specimen during the test in order to record the affected variable amplitude strain signals for both specimen and also the Charpy striker. Using the signal processing analysis for VA strain loading, the power spectrum density approach was used for determining the energy-based distribution. To obtain this type of energy, the VA strain signals were converted from the time domain to a frequency domain using the Fast Fourier Transform method. Significantly, the signal analysis showed that the AZ31B magnesium alloy with 0.2% CNT absorbed the highest amount of energy among the tested specimens. Therefore, addition of an optimal amount of CNTs improves the strength of alloys.

© 2015 Published by Elsevier Ltd. This is an open access article under the CC BY-NC-ND license (<http://creativecommons.org/licenses/by-nc-nd/4.0/>).

Peer-review under responsibility of the Czech Society for Mechanics

* Corresponding author. Tel.: +603 8911 8411; fax: +603 89118389.
E-mail address: shahrum@eng.ukm.my

Keywords: Carbon nanotube; Impact; Magnesium alloy; Power spectrum density, Transient load

1. Introduction

The demand for lightweight materials is particularly high for automotive applications because such materials can reduce vehicle loads and save on fuel costs [1]. One of the most important material properties is strength, which allows a device to withstand various impact circumstances. The development of composites has improved the current technology by introducing many lightweight polymer composite materials, and polymer composites feature several flaws in their material structures [2]. Thus, research attention has been diverted to magnesium alloys as lightweight materials. Most magnesium alloys used in the automotive and aerospace industries belong to the AZ31B alloy series; this series provides strength properties suitable for many applications [3].

AZ31B alloys can naturally withstand impacts effectively because of their unique combination of high tensile strength (up to 410 MPa), low density (1.8 g/cm³), and superior shock absorbency (100 times greater than that of ordinary aluminum alloys) [4]. Magnesium also has the highest specific damping capacity among the metals used in armor applications. Thus, the metal is an excellent choice for ballistic applications because of its enhanced energy absorption and shock mitigation. Magnesium has a hexagonal close-packed (HCP) structure. In HCP inorganic compounds, larger atoms (or ions) occupy positions corresponding approximately to those of equal spheres in close packing, while smaller atoms are distributed among the voids [5]. As such, a material that can fill these voids is necessary to prevent structure collapse. The most suitable material for filling such voids is carbon nanotubes (CNTs) with nano materials within the tubes. CNTs have unique properties that can generate strong materials and improve the energy absorption of a material [6–8], and many researchers acknowledge that CNTs can enhance the strength of a material. The molecular nanotechnology of CNTs can fill the spaces in a structure and produce van der Waals bonds therein [9–11].

AZ31B magnesium alloy is suitable for many impact applications, but the strength of the material can still be enhanced. Reinforcement of nano-sized particles is necessary to change the internal structure of the alloy and increase its strength, particularly in energy absorptive materials. This paper presents the variation in energy absorption of AZ31B magnesium alloys synthesized with different percentages of CNTs. Energy absorption was measured using signal-processing techniques that convert the strain signal into a time domain through Fast Fourier Transform (FFT) and a frequency domain through Power Spectrum Density (PSD). The results are vital for studying the effects of CNTs on the energy absorption and toughness of metal matrix composite materials.

2. Materials & Methods

2.1. Methodology

The methodology used for this study is shown in the flow diagram in Fig. 1. The sample was first prepared to enhance the determination of the energy absorption of magnesium alloys with increasing CNT composition. Measurement of energy absorption employed novel signal-processing methods [12].

Fig. 2 shows the machine used in the AZ31B magnesium alloy smelting process and the CNT size used. The CNTs used had a purity greater than 90%; their outer diameter was between 10 and 30 nm and their density was 2.1 g/cm³. CNTs were added to the sample at given proportions through a disintegrated melt deposition technique [13]. This technique employs high superheat temperatures and low impinging gas jet velocities, the end product of which is the bulk alloy only. Upon reaching a superheat temperature of 750 °C, the molten alloy melt was mechanically stirred using a mild steel impeller blade to facilitate the incorporation and uniform distribution of reinforcement materials into the metallic matrix.

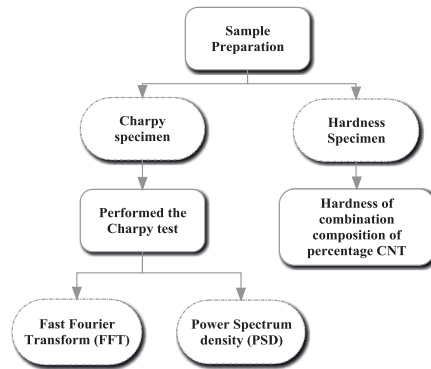


Fig. 1 Flow diagram of the methodology applied in the present work.

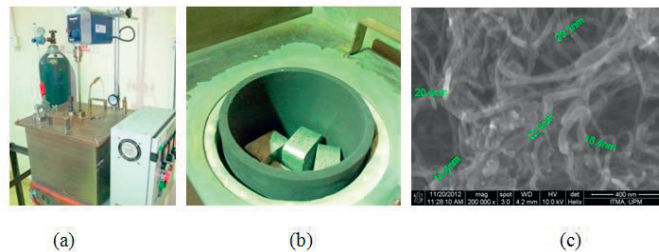


Fig. 2 (a) Vacuum induction furnace for melting magnesium. (b) AZ31B ingot on a crucible. (c) Size of the CNTs added to AZ31B.

The AZ31B magnesium alloy was melted, and different compositions of CNTs at 0.1%, 0.2%, and 0.5% were added to it. The added value of this composition was based on the level of equity mixture magnesium structure with CNT structure determined by previous researchers [14]. The composition percentage of AZ31B is shown in Table 1 and follows the ASTM B90 standard [15].

Table 1. Elemental composition (percentage) of AZ31B [15].

	Al	Mn	Zn	Ca	Composition %					Mg
					Cu	Fe	Ni	Si	Each	
AZ31B	2.5-3.5	0.2-1.0	0.6-1.4	0.04	0.05	0.005	0.005	0.10	0.30	Balance

2.2. Hardness Testing

A hardness test determined changes in the hardness of the alloys induced by the CNTs. The Rockwell hardness (RHL) test was performed using a 6.35 mm diameter steel ball with a total test force of 588.4 N, consistent with the ASTM E18 standards. The testing was intended to look the influenced of hardness by the addition of a particle such as CNT. In addition, that can show the contribute significance of the energy absorption with hardness.

2.3. Impact Testing

Fig. 3 shows the specimens used in the Charpy test and these specimens are prepared according to the ASTM E23 standard [16], allowing the validation of experimental results with quality standards. The testing was intended to look at energy absorption respond of the samples. Energy absorption of high energy reflects the ability of the study.

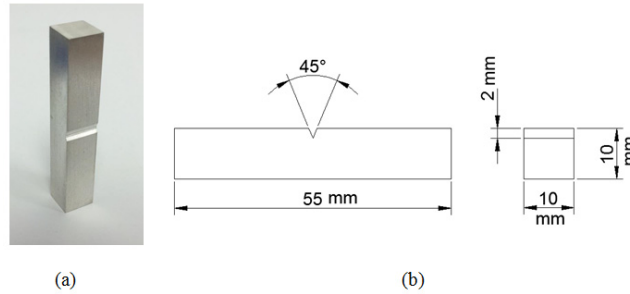


Fig. 3 (a) Charpy specimen. (b) Schematic diagram of the specimen according to ASTM E23 standard [16].

Prior to conducting the Charpy test, a strain gauge was attached to the back of the specimen receiving the optimal impact strain [17]. Fig. 4 shows the apparatus used to measure the strain signal and the specimen attached to the strain gauge. The strain gauge signal results were analyzed using the FFT method and transformed into a time domain. PSD was used to convert the energy results obtained. The frequency used to measure the strain data was 50 kHz; whose data suitability of the strain signal was not lost due to the high speed of the Charpy impact [17-19].

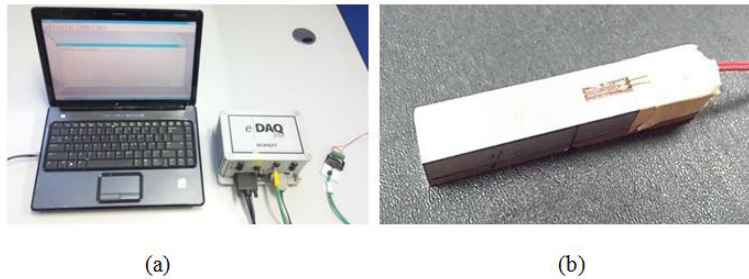


Fig. 4 (a) Data acquisition was used to receive the signal from the strain gauge at a 50 kHz frequency. (b) The position of the strain gauge in the specimens.

2.4. Application of a signal analysis approach

An approximation of the PSD matrix function of the response of a nonlinear multi-degree of freedom mechanical system with damping can be obtained by an equivalent linear system method, where the natural frequency is a random variable. The PSD matrix function of the non-linear response is defined as the PSD of the stationary response of the equivalent linear system. This approach involves a complicated numerical analysis when solving problems of the non-linear Eigen value produced (non-linear modes of vibrations) [18]. The autocorrelation function and the power spectrum have similar measurements in the time and frequency domains. Both of these functions can be related to the Fourier Transform Function, and PSD can be calculated using the following formula:

$$P_{xx}(\omega) = \frac{1}{2\pi} \int_{-\infty}^{\infty} r_{xx}(\tau) e^{-j\omega\tau} d\tau \quad (1)$$

The relationship between the autocorrelation functions is given as

$$r_{xx} = \int_{-\infty}^{\infty} x(t)x(t-\tau)dt \quad (2)$$

The autocorrelation function is usually an even function for τ , whereas the power spectrum function is usually an even function of ω . The imaginary parts $e^{j\omega}$ and $e^{-j\omega}$ are not considered in the integration procedure for each function. This integration is stated as

$$P_{xx}(\omega) = \frac{1}{2\pi} \int_{-\infty}^{\infty} r_{xx}(\tau) \cos(\omega\tau) d\tau \quad (3)$$

where

$$r_{xx}(\tau) = 1/2\pi \int P_{xx}(\omega) \cos(\omega\tau) d\omega \quad (4)$$

The power spectrum function $P_{xx}(\omega)$ provides information related to the average power for the signal component, and the frequency spectrum $G(j\omega)$ is a function of the amplitude and the phase angle. The relationship between $P_{xx}(\omega)$ and $G(j\omega)$ is

$$P_{xx} = |G(j\omega)|^2 \quad (5)$$

3. Results and Discussion

3.1. Hardness analysis

Fig. 5 shows the hardness of each alloy sample. The graph shows that the highest hardness was achieved by AZ31B, followed by the AZ31B + 0.2% CNT sample. The lowest hardness was achieved by the AZ31B + 0.1% CNT sample. However, the level of hardness, with a mixture of AZ31B with % CNT was around 91 to 96 RHL. This result shows that addition of CNTs causes no significant change in the hardness of the material. The same findings were observed by several researchers [6–9], who mentioned that the hardness of materials combined with CNTs remains fairly constant. However, the changing nature of hardness still exists slightly. Different hardness conditions alter the level of the total composition distribution acceptable for magnesium with CNT. Moreover, AZ31B + 0.2% CNT was the best mixture composition (Fig. 9). The energy absorption capabilities of this compound were subsequently impact-tested.

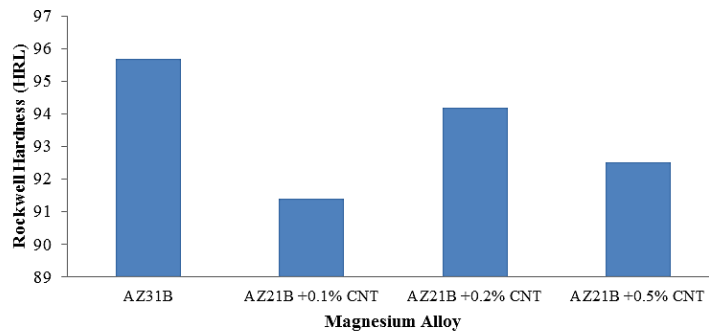


Fig. 5 Hardness of the different magnesium alloys

3.2. Impact Testing Analysis

The strain gauge attached to the rear of the specimen was used to obtain strain deformation signals. The strain signal was then analyzed using a signal processing method to measure the energy absorption of the specimens. Fig. 6 shows the graph formed by FFT of the signal yield strain. The results show that the highest microstrain (in the event of impact) was achieved by AZ31B + 0.2% CNT, followed by the original AZ31B alloy. The microstrains of AZ31B + 0.1% CNT and AZ31B + 0.5% CNT were approximately equal. The peak value of all materials tested was 48.8 Hz as shown as Fig. 6. The impact frequencies obtained were similar to those found by previous research [12]. These results indicate that the Charpy setup conditions in the present experiment were similar to those in standard conditions and that the impact and frequency of the Charpy experiment were uniform.

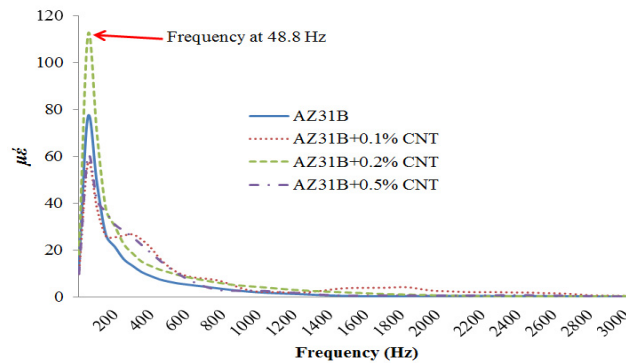


Fig. 6 The distribution of strain amplitude in the form of the FFT

Fig. 7 (a) shows the PSD plot produced by the materials tested. The PSD of AZ31B + 0.2% CNT was evidently the highest among the samples tested. The PSD is an important indicator in determining the level of energy that can be received by a substance. Fig. 7 (b) shows the energy that can be absorbed by the material being tested. Energy absorption was highest in AZ31B + 0.2% CNT, followed by AZ31B, AZ31B + 0.1% CNT, and AZ31B + 0.5% CNT.

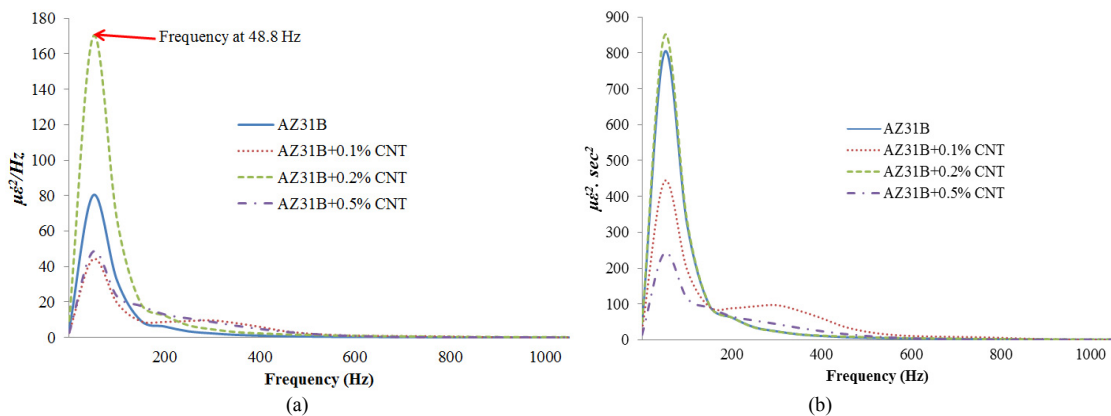


Fig. 7 (a) Distribution of the PSD among the different materials tested, (b) Distribution of energy absorbed during material testing.

3.3. Energy Absorption and Toughness of the Alloys

Addition of CNTs to the magnesium alloys improved their impact energy absorption and changed their toughness. However, the addition of CNT gives a lower impact energy absorption, if an optimal quantity is not given in the mixed of AZ31B alloy. The energy absorption of AZ31B + 0.1% CNT was lower than that of the original AZ31B alloy. This result indicates that addition of CNTs affected the blank voids to be filled by the CNTs which will avoid dislocation process. CNT content was not enough to cause an uneven internal structure of magnesium, which is susceptible to each molecule sliding. This also interferes with the van der Waals bond, which makes CNT weaker, because voids in the molecules are magnesium alloy.

The addition composition of CNT was larger than optimum value for the AZ31B + 0.5% CNT. Excess CNT content causes saturation in the structure of the material, which affects bonding interactions between atoms and produces structural materials that are prone to sliding. Dislocation at the beginning of structure failure is assumed. In this experiment, the optimum amount of CNTs added to magnesium alloy was 0.2% of the total CNT volume. This value was considered optimal for a given CNT volume, which was compatible with the empty voids in the structure of the magnesium alloy. This was evidenced by the level of energy absorption compared to the other experimental materials.

Energy absorption is closely related to the toughness of a material. Therefore, the toughness of a material has a significant relationship with its energy absorption. Toughness is linearly proportional to energy absorption (Equation 6) [19]:

$$\text{Toughness} = \frac{\text{Energy}}{\text{Area}} \quad (6)$$

The equation above shows that the toughness of a material has a significant relationship with energy absorption if the area of impact is consistent. Fig. 8 shows a graph correlating the energy absorption with the toughness of the materials used. In summary, differences in the energy absorption of AZ31B + 0.2% CNT are clearly visible between FFT, PSD and Energy graph. The energy absorption of AZ31B + 0.2% CNT is nearly twice that of AZ31B + 0.1% CNT and + AZ31B + 0.5% CNT.

Addition of CNTs to the alloys greatly improved their toughness but exerted limited effects on their hardness. Fig. 5 shows that the original AZ31B had the highest hardness among the samples examined.

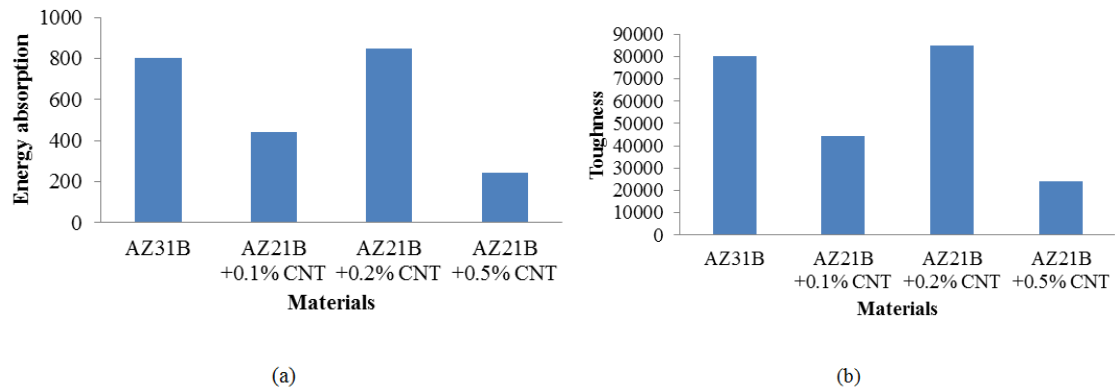


Fig. 8 Distributions of (a) energy absorption and (b) material toughness.

4. Conclusion

The use of lightweight materials is increasing in the automotive and aerospace industries. Although the use of magnesium alloys is widely accepted in the market, their strength characteristics may further be improved. This study combined AZ31B magnesium alloys with different amounts of CNTs, which improved the impact energy absorption of the resultant materials. The optimum additional amount of CNT is 0.2% of the total CNT volume compared to 0.1 and 0.5 % CNT. Addition of CNTs increased the optimal energy absorption of the alloys by 10%. The energy absorption obtained from AZ31B + 0.2% CNT approached twice that of AZ31B + 0.1% CNT and AZ31B + 0.5% CNT. The results obtained from addition of 0.2% CNT may be further improved by considering that the energy absorption of the material is subject to compression at a certain pressure. Certain pressures can change the shape of the grain boundary and make it more compact

Acknowledgements

The authors would like to express their gratitude to Ministry of Higher Education Malaysia via Universiti Kebangsaan Malaysia and Universiti Pertahanan Nasional Malaysia (Research funding: FRGS/1/2012/TK04/UPNM/0304 and LRGS/2013/UPNM-UKM/DS/04) for supporting this research.

References

- [1] Bakshi, S. R., Lahiri, D. and Agarwal, A. Carbon nanotube reinforced metal matrix composites – a review. *International Materials Reviews*. 2010 vol 55 (1). Pp 41-64.
- [2] El-Magd, E. and Abouridouane, M. Characterization, modelling and simulation of deformation and fracture behaviour of the light-weight wrought alloys under high strain rate loading. *International Journal of Impact Engineering* 32 (2006) pp 741–758.
- [3] Watari, H., Davey, K., Rasgado, M.T., Izawa, S., 2004, Semi-solid manufacturing process of magnesium alloy by twin-roll casting, *J. Material Processing Technology*, Vol 155-156: 1662-1667
- [4] Jones, T.L., Richard, D.D., Matthew, S.B., William, A.G., 2007, Ballistic performance of magnesium alloy AZ31B. 23rd Int. Sym. on Ballistics. Tarragona, Spain. Pp: 989-995.
- [5] Jena, P.K. K. S. Kumar, V. R. Krishna, A.K. Singh and T. B. Bhat. Studies on the role of microstructure on performance of a high strength armour steel. *Engineering Failure Analysis* 15 (2008) 1088–1096
- [6] Qianqian Li, Christian A. Rottmair, Robert F. Singer. CNT Reinforced Light Metal Composites Produced by Melt Stirring and by High Pressure Die Casting. *Composites Science and Technology* 2012. Pp 1-17.
- [7] Muhammad Rahman, Mahesh Hosur, Shaik Zainuddin, Uday Vaidya, Arefin Tauhid, Ashok Kumar, Jonathan Trovillion, Shaik Jeelani. Effects of amino-functionalized MWCNTs on ballistic impact performance of E-glass/epoxy composites using a spherical projectile. *International Journal of Impact Engineering* 57 (2013) 108-118.
- [8] Eslam M. Soliman, Michael P. Sheyka, Mahmoud Reda Taha. Low-velocity impact of thin woven carbon fabric composites incorporating multi-walled carbon nanotubes. *International Journal of Impact Engineering* 47 (2012) pp39-47.
- [9] Avila AF, Soares MI, Neto AS. A study on nanostructured laminated plates behaviour under low-velocity impact loadings. *Int J Impact Eng* 2007;34: 28-41
- [10] Patent N0.2 US 7,921,899 B2. Method for marking magnesium-based carbon nanotube composite material. United States Patent 2011. Pp 1-6.
- [11] Tan V, Ching T. Computational simulation of fabric armour subjected to ballistic impacts. *Int J Impact Eng* 2006;32:1737-51.
- [12] Ali, M. B., Abdullah, S., Nuawi M.Z. and Ariffin, A. K. Investigation of Energy Absorbed from an Instrumented Charpy Impact on Automotive Specimens. *Applied Mechanics and Materials* Vol. 165 (2012) pp 182-186
- [13] Nguyen, Q. B. and M. Gupta (2008) Increasing significantly the failure strain and work of fracture of solidification processed AZ31B using nano-Al₂O₃ particulates. *Journal of Alloys and Compounds*, 459(1–2), 244–250.
- [14] Katsuyoshi Kondoh, Hiroyuki Fukuda, Junko Umeda, Hisashi Imai, Bunshi Fugetsu, Morinobu Endo. Microstructural and mechanical analysis of carbon nanotube reinforced magnesium alloy powder composites. *Materials Science and Engineering A* 527 (2010) pp 4103–4108.
- [15] ASTM standard B90/B90M – 12: Standard Specification for Magnesium-Alloy Sheet and Plate. Pp: 1-8.
- [16] ASTM E23-02a. Standard Test Methods for Notched Bar Impact Testing of Metallic Materials. ASTM International. Pp 1-27.
- [17] Ali, M. B., Abdullah, S., Nuawi M.Z. and Ariffin, A. K. Analysis of an Instrumented Charpy Impact Using Power Spectrum Density. *Key Engineering Materials* Vols. 462–463 (2011) pp 130-135.
- [18] Shterenlikht, A., Hashemi, S. H., Yates, J R., Howard, I. C. and Andrews, R. M. 2005. Assessment of an Instrumented Charpy impact machine. *International Journal of Fracture* 132: 81-97.
- [19] Jang, Y.C., Hong, J.K., Park, J.H., Kim D.W. and Lee Y. 2008. Effects of notch position of the charpy impact specimen on the failure behaviour in heat affected zone. *Journal of materials processing technology* 201: 419–424.